

Highly efficient bilayer red phosphorescent organic light-emitting devices with solution-processed emission layer

DA-YOUNG PARK, MI-YOUNG HA, DAE-GYU MOON*

Department of Materials Engineering, Soonchunhyang University, 646, Eupnae-ri, Shinchang-myeon, Asan-si, Chungcheongnam-do, 336-745, Republic of Korea

We have developed highly efficient bilayer red phosphorescent organic light-emitting devices (OLEDs) using a solution-processed poly(N-vinylcarbazole) (PVK) host layer doped with tris(2-phenyl-1-quinoline)iridium(III) [Ir(phq)₃] molecules. PVK was mixed with Ir(phq)₃ molecules of 0.2 - 10 wt% in a chlorobenzene solution and spin-coated in order to prepare the emission layer. 3-(4-biphenyl)-4-phenyl-5-(4-tert-butylphenyl)-1,2,4-triazole (TAZ) was used as an electron transport material. The electrical conduction, emission, and efficiency characteristics of the OLEDs with a resultant structure of ITO/PVK:Ir(phq)₃/TAZ/LiF/Al were investigated. The maximum current efficiency and external quantum efficiency were 19.5 cd/A and 10.5%, respectively, in the device with 1% Ir(phq)₃ doped PVK host layer.

(Received June 29, 2017; accepted November 28, 2017)

Keywords: OLED, Phosphorescence, Solution processing, PVK

1. Introduction

Phosphorescent organic light-emitting devices (OLEDs) have attracted much attention in the past decades because they can realize highly efficient displays and solid-state lighting applications by harvesting both the electro-generated singlet and triplet excitons [1]. In particular, phosphorescent OLEDs based on polymer host layers have been extensively studied because they can provide low-cost, simple structure, and large area applications using simple solution processes, such as spin coating and inkjet printing [2]. Although many authors have demonstrated highly efficient phosphorescent OLEDs exhibiting a theoretical external quantum efficiency of about 20% using a vacuum evaporation method [3,4], the solution-processed devices require further improvement of efficiency and lifetime.

Poly(N-vinylcarbazole) (PVK) has been widely used as a polymer host for the phosphorescent OLEDs because it has excellent film forming property, high glass transition temperature, high triplet energy, and long lifetime of triplet excited states [5-8]. Since the PVK has a hole transporting property [9], electron transporting materials are required to balance the electrons and holes. The charge balance can be improved by mixing electron transporting materials with PVK host. For example, 2-(4-biphenyl)-5-(4-tert-butylphenyl)-1,3,4-oxadiazole (PBD) and 1,3-bis[(4-tert-butylphenyl)-1,3,4-oxadiazolyl]phenylene have been widely used as the blending materials [10,11]. Another method for improving the charge balance is to deposit additional electron transporting layer on top of the doped PVK layer [10]. In addition, the triplet energy level

of the electron transporting material should be higher than the phosphorescent guest emitter in order to confine the triplet excitons inside the emission layer [12,13].

In this paper, we report on bilayer phosphorescent OLEDs prepared by solution-processing of PVK host layer doped with red phosphorescent tris(2-phenylquinoline)iridium(III) [Ir(phq)₃] guest molecules. Although the Ir(phq)₃ has been known to be stable and efficient phosphor exhibiting a high phosphorescent quantum yield [14], there are very few reports on the solution-processed devices fabricated by using this phosphor as a guest emitter. We used 3-(4-biphenyl)-4-phenyl-5-(4-tert-butylphenyl)-1,2,4-triazole (TAZ) for electron transporting layer on top of the Ir(phq)₃ doped PVK layer because the TAZ has a high triplet energy and a good hole blocking property [15]. Based on the investigation of the electrical conduction, carrier recombination, energy transfer, and emission properties of the devices by varying Ir(phq)₃ concentration, we demonstrated highly efficient bilayer red phosphorescent devices with solution-processed PVK:Ir(phq)₃ layer.

2. Experimental

Indium tin oxide coated glass substrates were used for the preparation of the bilayer red phosphorescent OLEDs. The sheet resistance of the ITO film was about 10 Ω/□. The ITO film was patterned to define anode electrodes by using photolithography processes and the substrates were cleaned with isopropyl alcohol, methanol, and deionized water. The cleaned substrates were treated with oxygen

plasma at 10 W for 3 min before spin-coating of the solutions prepared by mixing $\text{Ir}(\text{phq})_3$ with PVK in a chlorobenzene solution at room temperature. The concentration of $\text{Ir}(\text{phq})_3$ was varied from 0.2 to 10 wt%. The thickness of the doped PVK layer was 50 nm. After the preparation of $\text{Ir}(\text{phq})_3$ doped PVK layer which acts as hole transporting and emission layer, a 50 nm thick TAZ electron transporting layer was deposited by using a vacuum thermal evaporation method at a base pressure of about 1×10^{-6} Torr. After coating of organic layers, a 0.5 nm thick LiF and a 100 nm thick Al layers were sequentially evaporated through a shadow mask for the formation of cathode. The completed device structure was ITO/PVK: $\text{Ir}(\text{phq})_3$ (50 nm, 0.2 - 10 wt%)/TAZ (50 nm)/LiF (0.5 nm)/Al (100 nm). The active area of the devices was $4 \times 4 \text{ mm}^2$. Current density-voltage-luminance characteristics of the devices were measured using computer controlled Keithley 2400 source-measure units and a calibrated fast Si photodiode. The electroluminescence (EL) spectra of the devices were measured by a spectroradiometer (Minolta CS1000).

3. Results and discussion

Fig. 1 shows the current density curves as a function of voltage for the red phosphorescent OLEDs with a bilayer structure of ITO/PVK: $\text{Ir}(\text{phq})_3$ /TAZ/LiF/Al. The concentration of $\text{Ir}(\text{phq})_3$ was varied from 0.2 to 10 wt%. Chao et al. demonstrated the mixed host structure of PVK, PBD, and N,N'-diphenyl-N,N'-bis(3-methylphenyl)-1,1'-biphenyl-4,4'-diamine (TPD) as a host of $\text{Ir}(\text{phq})_3$ guest emitter [16]. They reported that the solubility of $\text{Ir}(\text{phq})_3$ was less than 0.1 wt% in a mixed solution of PVK, PBD, and TPD dissolved in a chlorobenzene solvent. In our case, only PVK was used as a host so that the $\text{Ir}(\text{phq})_3$ could be dissolved uniformly up to 10 wt% in a PVK solution at room temperature. The driving voltage increases as the $\text{Ir}(\text{phq})_3$ concentration increases from 0.2 to 5 wt%. For example, the required voltages for achieving a current density of 10 mA/cm^2 are 11.4 and 16 V, respectively, in the 0.2 and 5 wt% $\text{Ir}(\text{phq})_3$ devices. On the other hand, the driving voltage of the 10 wt% $\text{Ir}(\text{phq})_3$ device is lower than that of the 5 wt% $\text{Ir}(\text{phq})_3$ device. For example, the driving voltage for a current density of 10 mA/cm^2 is 14.2 V. This result indicates that the $\text{Ir}(\text{phq})_3$ molecules in a PVK host act as trap sites for carriers [17]. The highest occupied molecular orbital (HOMO) and the lowest unoccupied molecular orbital (LUMO) energy levels of $\text{Ir}(\text{phq})_3$ are 5.0 and 2.8 eV, respectively [4]. The HOMO and LUMO levels of PVK are 5.8 and 2.2 eV, respectively [7]. The electrons and holes can be trapped on the $\text{Ir}(\text{phq})_3$ molecules in a PVK host since the HOMO and LUMO levels of $\text{Ir}(\text{phq})_3$ are located within the energy gap of PVK. The holes are likely to be trapped on the guest molecules because the electron-hole recombination takes place in the emission layer adjacent to the TAZ electron transport layer due to the strong hole-blocking property of the TAZ [15]. At $\text{Ir}(\text{phq})_3$ concentration of 0.2 - 5 wt%, the

increase of driving voltage with increasing $\text{Ir}(\text{phq})_3$ concentration indicates that the current conduction is determined by the emission of trapped carriers from $\text{Ir}(\text{phq})_3$ guest to the PVK host molecules. The distance between the trap sites becomes shorter in the 10 wt% $\text{Ir}(\text{phq})_3$ devices so that the carriers are transported by hopping between $\text{Ir}(\text{phq})_3$ molecules, resulting in lowering of driving voltage compared with the 5 wt% $\text{Ir}(\text{phq})_3$ device. In addition, the carriers can be directly injected onto the $\text{Ir}(\text{phq})_3$ molecules at 10 wt% $\text{Ir}(\text{phq})_3$ concentration because of the increased population of these molecules at the anode/emission layer and emission layer/TAZ interfaces.

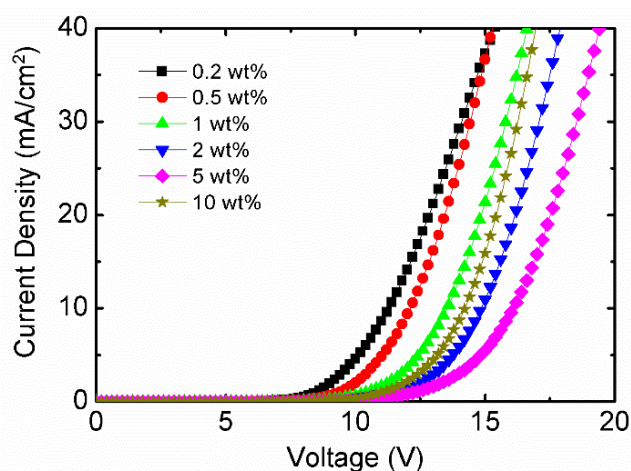


Fig. 1. Current density curves as a function of voltage for the red phosphorescent OLEDs with various $\text{Ir}(\text{phq})_3$ concentrations

Fig. 2 shows the luminance curves as a function of voltage for the devices with various $\text{Ir}(\text{phq})_3$ concentrations. The turn-on voltage which is defined as a required voltage for achieving a luminance level of 0.1 cd/m^2 is about 5.0 V at 0.2 wt% $\text{Ir}(\text{phq})_3$ concentration. The turn-on voltage slightly decreases to 5.4 V as the $\text{Ir}(\text{phq})_3$ concentration increases to 5 wt%. Further increase of $\text{Ir}(\text{phq})_3$ concentration to 10 wt% results in slight decrease of turn-on voltage to 5.2 V. The luminance dependence on the $\text{Ir}(\text{phq})_3$ concentration at higher voltage also exhibits the same tendency as the turn-on voltage dependence. For example, the luminance at 10 V decreases from 318.8 to 30.9 cd/m^2 as the $\text{Ir}(\text{phq})_3$ concentration increases from 0.2 to 5 wt%. After then, the luminance increases to 72.9 cd/m^2 as the $\text{Ir}(\text{phq})_3$ concentration increases to 10 wt%. Since the luminance is determined by the driving current and current efficiency, this luminance dependence on the $\text{Ir}(\text{phq})_3$ concentration reflects the modification of carrier transport by the $\text{Ir}(\text{phq})_3$ molecules acting as carrier trap sites.

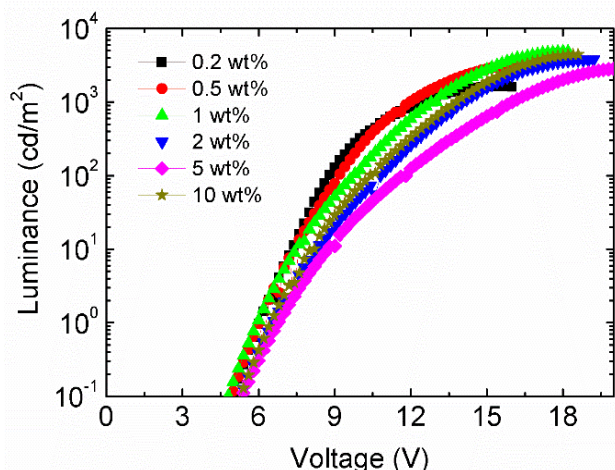


Fig. 2. Luminance curves as a function of voltage for the red phosphorescent OLEDs with various $\text{Ir}(\text{phq})_3$ concentrations

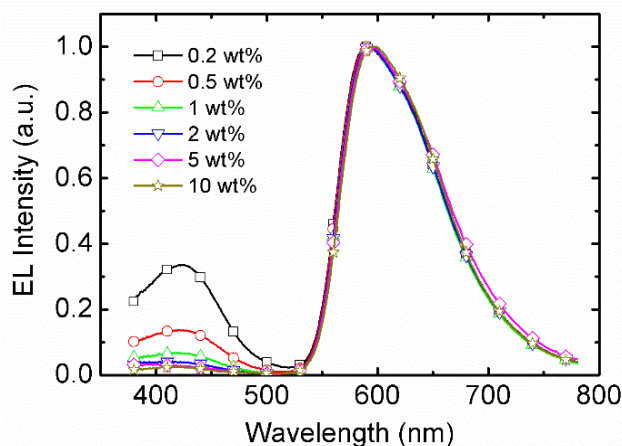


Fig. 3. EL spectra measured at a voltage of 10 V for the red phosphorescent devices with various $\text{Ir}(\text{phq})_3$ concentrations.

Fig. 3 shows the EL spectra measured at a voltage of 10 V for the devices with various concentrations of $\text{Ir}(\text{phq})_3$ molecules. The devices exhibit the strong emission at 595 nm and the second emission at about 425 nm, corresponding to the emissions from $\text{Ir}(\text{phq})_3$ and PVK molecules, respectively [18,19]. The relative intensity of PVK emission is the highest at 0.2 wt% $\text{Ir}(\text{phq})_3$ concentration, decreasing with increasing $\text{Ir}(\text{phq})_3$ concentration. For example, the emission intensities at 425 nm are 0.34 and 0.02 at 0.2 and 10 wt%, respectively. The emission from the $\text{Ir}(\text{phq})_3$ guest molecules can be attributed to the energy transfer from the PVK host and/or direct recombination of electrons and holes on the guest molecules. Lamansky et al. reported that the excitons are generated by direct recombination on the guest molecules in the PVK:PBD hosted red phosphorescent devices [10]. The host emission was not observed in their PVK:PBD host devices. Gong et al. also reported that they could not observe the host emission even at very low dopant concentration of 0.02 wt% in the PVK:PBD hosted red phosphorescent devices, attributed to the direct recombination [20,21]. On the other hand, Noh et al. reported that the guest emission can be resulted from both the energy transfer and direct recombination in the PVK hosted green phosphorescent OLEDs [22]. In our devices, the $\text{Ir}(\text{phq})_3$ molecules act as traps for the carriers. These traps contribute to the direct exciton formation on the $\text{Ir}(\text{phq})_3$ guest molecules. In addition, the noticeable emission from PVK host indicates that the energy transfer also plays an important role to the emission from $\text{Ir}(\text{phq})_3$ guest molecules.

Fig. 4 shows the EL intensity at 425 nm as a function of driving voltage for the devices with various $\text{Ir}(\text{phq})_3$ concentrations. In the 0.2 wt% $\text{Ir}(\text{phq})_3$ device, the emission intensity decreases from 0.41 to 0.28 as the driving voltage increases from 7 to 13 V. This result excludes that the PVK emission at 425 nm may be attributed to the emission site saturation by the low $\text{Ir}(\text{phq})_3$ concentration. The site-saturated device exhibits opposite tendency that the intensity of host emission increases with increasing the driving voltage [23]. The result also indicates that the incomplete energy transfer from PVK host to $\text{Ir}(\text{phq})_3$ guest occurs in the 0.2 wt% $\text{Ir}(\text{phq})_3$ device. The distance between $\text{Ir}(\text{phq})_3$ guest molecules is too large to efficiently transfer the energy of excitons from the host to the guest molecules at low voltage in the 0.2 wt% device, so that the emission from PVK host is high at low voltage. As the driving voltage increases, the distance between the excited host and the guest molecules decreases due to the increased density of excitons in the PVK host, resulting in a decrease of host emission by the enhanced transfer of exciton energy to the guest molecules. On the other hand, the emission intensity as the driving voltage is not significantly modified in the 0.5 - 10 wt% $\text{Ir}(\text{phq})_3$ devices. For example, 1 wt% $\text{Ir}(\text{phq})_3$ device exhibits the PVK emission intensities of 0.06-0.07 at voltage ranges of 8 - 13 V. It indicates that the excited host - guest distance is enough to efficiently transfer the exciton energy from PVK host to the $\text{Ir}(\text{phq})_3$ guest molecules. In addition to the enhanced energy transfer, the increased direct recombination results in a weak dependence of emission intensity on the voltage in the 0.5 - 10 wt% $\text{Ir}(\text{phq})_3$ devices.

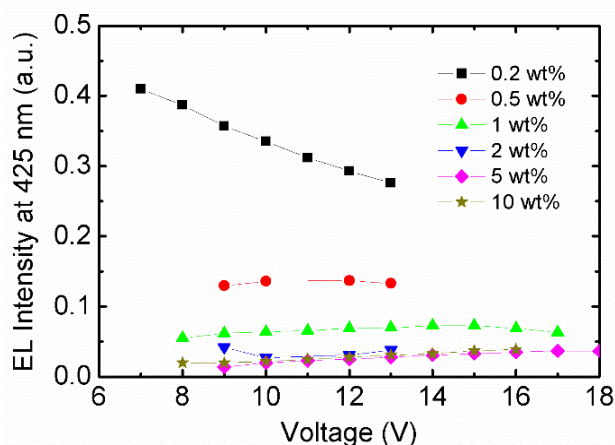


Fig. 4. The EL intensities at 425 nm as a function of voltage for the red phosphorescent devices with various $\text{Ir}(\text{phq})_3$ concentrations.

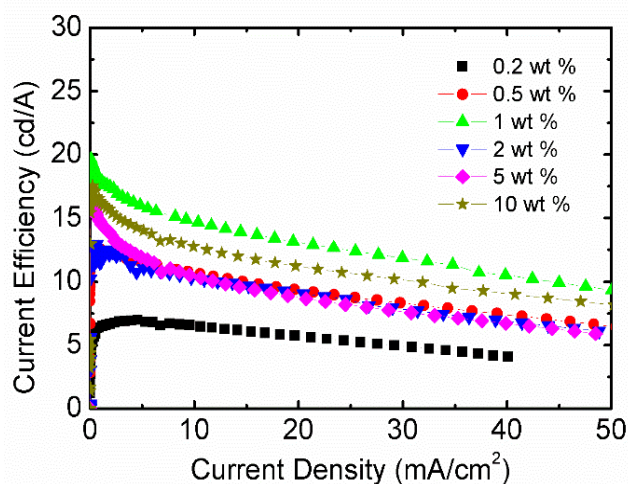


Fig. 5. Current efficiency curves as a function of current density for the red phosphorescent devices with various $\text{Ir}(\text{phq})_3$ concentrations.

Fig. 5 shows the current efficiency curves as a function of current density for the devices with various $\text{Ir}(\text{phq})_3$ concentrations. The 0.2 wt% $\text{Ir}(\text{phq})_3$ device exhibits low current efficiency due to the incomplete energy transfer from the PVK host to the $\text{Ir}(\text{phq})_3$ guest molecules. For example, the current efficiency is 6.5 cd/A at a current density of 10 mA/cm². As the $\text{Ir}(\text{phq})_3$ concentration increases to 1 wt%, the current efficiency increases to 14.7 cd/A at the same current density by the enhanced energy transfer. The maximum current efficiency reaches to 19.5 cd/A, corresponding to the maximum external quantum efficiency of 10.5% at a current density of 0.12 mA/cm². Further increase of $\text{Ir}(\text{phq})_3$ concentration to 5 wt% results in a decrease of current efficiency due to the drop of recombination efficiency as the $\text{Ir}(\text{phq})_3$ acts as carrier traps. At 10 wt% $\text{Ir}(\text{phq})_3$ concentration, the hopping of carriers via $\text{Ir}(\text{phq})_3$

molecules results in a slight increase of current efficiency. For example, the current efficiency increases from 10.5 to 12.8 cd/A as the $\text{Ir}(\text{phq})_3$ concentration increases from 5 to 10 wt%.

4. Conclusions

We have demonstrated highly efficient red phosphorescent OLEDs using a spin-coated PVK host layer doped with 0.2 - 10 wt% $\text{Ir}(\text{phq})_3$ guest molecules. The driving voltage increases with increasing $\text{Ir}(\text{phq})_3$ concentration up to 5 wt% as the $\text{Ir}(\text{phq})_3$ acts as traps for carriers. On the other hand, the driving voltage of 10 wt% $\text{Ir}(\text{phq})_3$ device is lower than the 5 wt% device, as the carrier transport is dominated by hopping via $\text{Ir}(\text{phq})_3$ molecules. The emission from PVK host decreases with increasing $\text{Ir}(\text{phq})_3$ concentration, due to both the enhanced energy transfer from host to guest molecules and the increased direct recombination on the $\text{Ir}(\text{phq})_3$ guest molecules. Due to these energy transfer and direct recombination, the current efficiency was determined by the energy transfer efficiency and the charge balance. The 1 wt% $\text{Ir}(\text{phq})_3$ device exhibited the maximum current efficiency of 19.5 cd/A and external quantum efficiency of 10.5%.

Acknowledgements

This work was supported by the Soonchunhyang University Research Fund and by the Global Leading Technology Program (10042477) of MOTIE/KEIT.

References

- [1] M. A. Baldo, D. F. O'Brien, Y. You, A. Shoustikov, S. Sibley, M. E. Thompson, S. R. Forrest, *Nature* **395**, 151 (1998).
- [2] V. Cleave, G. Yahioglu, P. Barny, R. H. Friend, N. Tessler, *Adv. Mater.* **4**, 285 (1999).
- [3] S. Su, T. Chiba, T. Takeda, J. Kido, *Adv. Mater.* **20**, 2125 (2008).
- [4] J. H. Jou, S. H. Shen, S. H. Chen, M. H. Wu, W. B. Wang, H. C. Wang, C. R. Lin, Y. C. Chou, P. H. Wu, J. J. Shyue, *Appl. Phys. Lett.* **96**, 143306 (2010).
- [5] K. S. Yook, J. Y. Lee, *Adv. Mater.* **26**, 4218 (2014).
- [6] C. L. Lee, K. B. Lee, J. J. Kim, *J. Appl. Phys.* **77**, 2280 (2000).
- [7] Y. Kawamura, S. Yanagida, S. R. Forrest, *J. Appl. Phys.* **92**, 87 (2002).
- [8] J. Pina, J. Melo, H. D. Burrows, A. P. Monkman, S. Navaratnam, *Chem. Phys. Lett.* **400**, 441 (2004).
- [9] W. D. Gill, *J. Appl. Phys.* **43**, 5033 (1972).
- [10] S. Lamansky, R. C. Kwong, M. Nugent, P. I. Djurovich, M. E. Thompson, *Org. Electron.* **2**, 53 (2001).

- [11] X. Yang, D. C. Müller, D. Neher, K. Meerholz, *Adv. Mater.* **18**, 948 (2006).
- [12] K. Goushi, R. Kwong, J. J. Brown, H. Sasabe, C. Adachi, *J. Appl. Phys.* **95**, 7798 (2004).
- [13] I. Tanaka, Y. Tabata, and S. Tokito, *Chem. Phys. Lett.* **400**, 86 (2004).
- [14] A. Endo, C. Adachi, *Chem. Phys. Lett.* **483**, 224 (2009).
- [15] L. Xiao, S. J. Su, Y. Agata, H. Lan, J. Kido, *Adv. Mater.* **21**, 1271 (2009).
- [16] Y. C. Chao, S. Y. Huang, C. Y. Chen, Y. F. Chang, H. F. Meng, F. W. Yen, I. F. Lin, H. W. Zan, S. F. Horng, *Synth. Met.* **161**, 148 (2011).
- [17] H. Murata, C. D. Merritt, Z. H. Kafafi, *IEEE J. Sel. Top. Quantum Electron.* **4**, 119 (1998).
- [18] K. Saito, N. Matsushita, H. Kanno, Y. Hamada, H. Takahashi, T. Matsumura, *Jpn. J. Appl. Phys.* **43**, 2733 (2004).
- [19] S. Kan, X. Liu, F. Shen, J. Zhang, Y. Ma, G. Zhang, Y. Wang, J. Shen, *Adv. Funct. Mater.* **13**, 603 (2003).
- [20] X. Gong, J. C. Ostrowski, G. C. Bazan, D. Moses, A. J. Heeger, *Appl. Phys. Lett.* **81**, 3711 (2002).
- [21] X. Gong, J. C. Ostrowski, D. Moses, G. C. Bazan, A. J. Heeger, *Adv. Funct. Mater.* **13**, 439 (2003).
- [22] Y. Y. Noh, C. L. Lee, J. J. Kim, K. Yase, *J. Chem. Phys.* **118**, 2853 (2003).
- [23] T. Tsuzuki and S. Tokito, *Adv. Mater.* **19**, 276 (2007).

*Corresponding author: dgmoon@sch.ac.kr